Inflammation, Vol. 43, No. 2, April 2020 (© 2019)
DOI: 10.1007/s10753-019-01152-5

ORIGINAL ARTICLE

Toll-Like Receptor 2–Mediated Autophagy Promotes Microglial Cell Death by Modulating the Microglial M1/M2 Phenotype

Kun Ma,[1,2] Jingjing Guo,[3] Guan Wang,[1] Qiuying Ni,[2] and Xinjie Liu[1,4]

Abstract— Toll-like receptor 2 (TLR2) regulates the innate immune response of microglia during infection *via* autophagy. Microglial M1/M2 phenotypic switching after infection could serve as a novel pathogenic mechanism for cerebral infection. Hence, it has important implications for the damage and restoration of neurological function. However, the effect of TLR2-mediated autophagic signaling on microglial phenotypic transition remains unclear. Therefore, we investigated the mechanisms of TLR2-mediated autophagic signaling in the regulation of microglial M1/M2 phenotypes. Using Western blot analysis and immunofluorescence, increased autophagy was observed in peptidoglycan (PGN)-stimulated BV2 cells, while reduced autophagy was observed in TLR2-KO cells. In contrast to the TLR2 antagonist CU-CPT22 group, increased autophagy was observed in the presence of the TLR2 agonist Pam3CSK4, which was associated with a significant increase in expression levels of M1 phenotype biomarkers (CD86, TNF-α, IL-6), higher levels of apoptosis, and decreased expression levels of M2 markers (CD206, IL-10, Arg-1). In the TLR2-KO mice, the expression levels of autophagy-related proteins in $CD11b^+$ cells were lower than those in $CD11b^+$ cells in the PGN-injected wild-type mice, and neuronal apoptosis was also reduced, but there were no significant differences compared to the control group. Collectively, our study demonstrates that the inhibition of autophagy or the absence of TLR2 induces microglial polarization towards the M2 phenotype, promotes microglial survival alone, and alleviates the development of neuroinflammation. In summary, TLR2-mediated autophagic signaling contributes to regulating the inflammatory response to activate microglial M1/M2 switching, which affects

Main Points • Transition from the M1 to the M2 phenotype promotes microglial survival.

• Autophagy is associated with the M1 phenotype and increased apoptosis.

• Inhibition or absence of TLR2 is associated with reduced autophagy.

[1] Department of Pediatrics, Qilu Hospital, Shandong University, No. 107, Wen Hua Xi Road, Jinan, 250012, Shandong, China
[2] The First Affiliated Hospital of Shandong First Medical University, Jinan, Shandong, China
[3] Central Hospital Affiliated to Shandong First Medical University, Jinan, Shandong, China
[4] To whom correspondence should be addressed at Department of Pediatrics, Qilu Hospital, Shandong University, No. 107, Wen Hua Xi Road, Jinan, 250012, Shandong, China. E-mail: doctorma2017@163.com

microglial survival after infection.

KEY WORDS: Toll-like receptor 2; autophagy; microglial phenotype transition; peptidoglycan.

INTRODUCTION

Microglia are the major immune cells in the brain that act as the first defense of the central nervous system. Upon infection, trauma, or ischemia, microglia can be rapidly activated, contributing to the inflammatory response. Activated microglia show a wide range of diverse functional states, mainly including pro-inflammatory M1 and anti-inflammatory M2 subtypes [1–4]. In many pathophysiological processes, microglia play a dual role through phenotypic switching. After injury, microglia quickly change their phenotype to secrete a large and diverse range of molecules that mediate inflammation. The M1 phenotype represents a detrimental state of microglia and is characterized by the high expression of pro-inflammatory mediators, such as tumor necrosis factor-α (TNF-α), interleukin (IL)-1, and IL-6, while the M2 phenotype is characterized by high levels of anti-inflammatory mediators, such as IL-10, IL-4, and arginase-1 (Arg-1) [5–7]. Moreover, the M1-like phenotype is characterized by an increased expression of surface markers, such as CD16/32, CD86, and CD40, while increased expression of CD206 is correlated with the M2 phenotype [8–10]. However, the mechanism underlying the switching of the microglial phenotype under infection conditions is still unclear.

Autophagy is a fundamental cellular homeostatic mechanism that is important for the control of inflammatory responses in the CNS and neurotoxicity [11, 12]. Autophagy is also a highly conserved process in which damaged and aging organelles and misfolded and denatured proteins are delivered to lysosomes for degradation and recycling of their functional blocks through anabolic reactions [13–15]. Autophagy plays a dual role in cancer, where it can prevent tumor initiation *via* its quality control function or can sustain tumor metabolism and survival *via* nutrient recycling [16]. During periods of starvation, stimulation of autophagy is important to provide cells with amino acids and fatty acids to maintain the level of cell metabolism [17, 18]. In a mouse model of Alzheimer's disease (AD) pathology, autophagy efficiency has demonstrated promising therapeutic effects on neuronal function and cognitive performance [19]. The interactions between autophagy proteins and immune signaling molecules are much more complex. Autophagy-associated proteins can either induce or inhibit immune and inflammatory responses, and immune and inflammatory signals can also regulate autophagy [20, 21]. A recent study found that autophagy is associated with microglial phenotypic transformation [3]. However, whether autophagy participates in the switching of the microglial phenotype following cerebral infection is unknown.

Toll-like receptors (TLRs) are highly expressed in multiple cell types in the CNS, such as the microglia, neurons, and astrocytes. TLRs represent the first point of contact between the organism and the environment, and for this reason, altering the activity or the expression of specific TLRs could reduce or prevent the development of diseases associated with an inflammatory status [22–24]. Animal studies have shown that Toll-like receptor 2 (TLR2)-knockout (KO) mice are more susceptible to meningitis due to *Streptococcus pneumonia* and infection with *Mycobacterium tuberculosis* [25]. Moreover, we observed that activation of microglial cells with peptidoglycan (PGN) results in cell activation followed by the induction of autophagy and autophagy-dependent cell death [26]. However, it is unknown whether autophagy alters the microglial phenotype through the TLR2 signaling pathway.

Despite the increasing reports studying the effects of autophagy on microglial phenotypic switching under various pathological conditions, little emphasis has been placed on microglial cells during infection. In this study, using *in vivo* mice models and *in vitro* assays, we investigated the relationship between autophagy and the TLR2 pathway in microglial cells treated with PGN. Then, we examined the effect of autophagic flux on the alternation of the BV2 microglial phenotype and its effect on cell survival.

MATERIALS AND METHODS

BV2 Cell Culture

The mouse microglia BV2 cell line (Central Laboratory of Shandong University Medical College, China) was cultured in Dulbecco's modified Eagle's medium (DMEM; HyClone, USA) containing 10% fetal bovine serum and penicillin-streptomycin (100 U/ml; 0.1 mg/ml) at 37 °C in a 5% CO_2-humidified incubator. Cells were trypsinized

(0.25% trypsin; Invitrogen, Thermo Fisher Scientific, USA) after entry into logarithmic growth phase to obtain single cell suspensions, which were subsequently seeded into 6-well plates (100 μl of 2×10^5 cells/well; Eppendorf, USA) for the signaling experiments. The cells were divided into 4 treatment groups: phosphate-buffered saline (PBS), PGN, PGN + CU-CPT22 (TLR2 antagonist; Sigma, Merck, USA), and PGN + Pam3CSK4 (TLR2 agonist; APExBIO, USA).

TLR2 Small Interfering RNA and Transfection

Three isoforms of TLR2 mRNA sequences were screened to select the small interfering RNA (siRNA) sequence to inhibit TLR2 expression. BV2 cell culture medium was replaced with fresh complete medium 2 h before transfection. The siRNA sequences (Guangzhou Ruibo Biotech Co., Ltd., China) were inserted into the plasmids (containing siRNA and empty vector) and were subsequently transfected into BV2 cells in the logarithmic phase using Lipofectamine 2000 (Invitrogen, Thermo Fisher Scientific, USA). The cells were cultured for 6 h before refreshing the culture medium, and growth continued for another 48 h. Western blot analysis was performed to verify TLR2 knockdown in the cells transfected with siTLR2 as previously described [25]. The siRNA that induced the greatest knockdown efficiency was selected for subsequent experiments. The anti-TLR2 antibody for Western blot analysis was purchased from Merck (USA).

Western Blot Analysis

PGN-treated BV2 cells were harvested and then lysed with RIPA buffer (Sigma, USA) containing a protease inhibitor on ice to obtain a total cell lysate. The protein concentration of the cell lysate was determined using a BCA assay (Biyuntian Biotechnology Co., Ltd., China). Proteins (20 μg) were separated using 10% SDS-PAGE and then transferred to nitrocellulose membranes (Millipore, MA, USA). The blots were incubated with anti-mouse LC3 (PTG; Sanying Biotechnology, Wuhan, China), rabbit anti-mouse Beclin-1 (Affinity Biosciences, Cincinnati, OH, USA), anti-TLR2 (Merck, USA), and anti-mouse GAPDH (Abcam, USA) primary antibodies at 4 °C overnight followed by incubation with horseradish peroxidase–conjugated goat anti-rabbit or goat anti-mouse (Merck, USA) secondary antibodies for 1 h at room temperature. The bands were then developed using an enhanced chemiluminescence reagent (Merck, USA) and were analyzed using ImageJ software.

ELISA to Detect Cytokine Expression Levels

ELISA was performed to determine the level of cytokine secretion from the PGN-treated BV2 cells. The protein lysate of the BV2 cells treated with PGN for 24 h was labeled using an ELISA cytokine detection kit (MultiSciences, China) and a CD206 and CD86 receptor detection kit (USCN, Wuhan, China). Absorbance values of TNF-α, IL-6, CD86, IL-10, Arg-1, and CD206 cytokines were obtained at 450 nm using a microplate reader (Bio-Rad, USA).

Flow Cytometry

Cells were cultured for 24 h and then harvested in ice-cold PBS at 4 °C for flow cytometry analysis to assess microglial survival under different conditions. Annexin V-FITC/PI staining solution (10 μl; BD, NJ, USA) was added to 100 μl of a 1×10^6/ml cell suspension in binding buffer in a 5-ml flow tube and incubated at room temperature for 15 min in the dark. After adding 400 μl of PBS to the flow tube, the suspension was analyzed using a flow cytometer (BD, USA).

Immunofluorescence

PGN and non-PGN-treated microglia grown on microscope slides were fixed with 4% paraformaldehyde for 10 min at room temperature, washed twice with PBS, and then incubated in 5% normal goat serum (Gibco; Thermo Fisher Scientific, USA). The slides were then incubated with 0.05% Tween 20 (Sigma, USA) for 1 h to reduce nonspecific binding before incubation with anti-LC3B and anti-LAMP-1 primary antibodies for 1 h at room temperature. Next, three washes with PBS were performed, followed by incubation with secondary antibody for 1 h and examination under an LSM780 fluorescence microscope (Zeiss, Germany).

Animal Handling and Grouping

Twelve 6–8-week-old male specific pathogen-free (SPF) grade C57BL/6J mice (Central Laboratory of Shandong University Medical College, China), weighing 20 ± 2.5 g, were randomly divided into four groups ($n = 3$; PBS, PGN, PGN + 3-methyladenine (3-MA), and PGN + siRNA-(si)TLR2 lentivirus groups) and were housed in separate well-ventilated cages at 20–25 °C with a relative humidity of 45–55% under a 12-h day/night cycle. The mice were given food and water *ad libitum*. Regular cleaning and disinfection of the cages were performed to ensure that the breeding environment was pathogen-free,

clean, and comfortable. The experiments complied with the Regulations of the Administration of Laboratory Animals of the Ministry of Health of China (Document No. 55 of 2001) and were approved by the Animal Ethics Committee of Shandong University, China. The *Staphylococcus aureus* extracts PGN and 3-MA were purchased from Sigma (Merck, USA). The lentivirus for siRNA transfection was purchased from Hanheng Biotechnology, China.

TLR2-KO Mouse Model

To establish the TLR2-KO model, mice were anesthetized with 0.75 mg/10 g of sodium pentobarbital (China Pharmaceutical Group Shanghai Chemical Reagent Company, China) and then fixed on a stereotaxic instrument. After disinfection, the skin on the top of the head was cut in the middle, and a 0.8-mm-diameter drill bit was used to expose the anterior fontanelle of the brain (1.5 mm opening). Then, si-TLR2 lentivirus (Heyuan Biotechnology Co., Ltd., China) was injected into the lateral ventricle according to the positioning coordinates: 1.7 mm depth and 0.6 mm after the anterior fontanelle. The skin was disinfected and sutured after the injection. The surgery was performed quickly under anesthesia to minimize discomfort and unnecessary injury to the mice. The surgery was performed in accordance with the Animal Management Regulations (School of Medicine, Shandong University, China).

Histoimmunofluorescence

One week after establishing the TLR2-KO model, mice were injected with the test agents (3.8×10^9 PFU/ml si-TLR2 lentivirus, 5 μg PGN, 0.5 μg 3-MA, and 5 μl PBS) *via* the same method as described for establishing the TLR2-KO model. The mice were sacrificed after 48 h by cutting the cervical vertebrae and the occipital bone from the back with scissors, and the brain was rapidly removed. Brain tissue sections (5 μm thickness) were subsequently paraffinized and routinely dewaxed in water, and antigen retrieval was performed *via* microwave treatment. The tissue sections were next soaked in 3% hydrogen peroxide solution for 10 min before incubation with rabbit anti-CD11b (Wuhan Yun Clone, China) and mouse anti-LC3B (CST, USA) primary antibodies overnight at 4 °C. Next, FITC-labeled LC3B (green) and A555-labeled CD11b (red) secondary antibodies (Invitrogen; Thermo Fisher Scientific, USA) were added dropwise and were incubated at 37 °C for 30 min before counterstaining with DAPI (Sigma, USA) at room temperature for 10 min. Finally, an anti-fluorescence quencher (Biyuntian Biotechnology Co., Ltd., China) was added dropwise before sealing with a coverslip. The expression pattern of the microglia-specific marker CD11b and autophagy protein LC3B were observed using confocal fluorescence microscopy (Olympus, Japan) at × 400 magnification. Three random sections in three different fields were selected to count the number of positively stained autophagic microglial cells. Image analysis was performed using Image-Pro Plus 6.0 software (Media Cybernetics, USA).

Nissl Staining

Brain hippocampal 4-μm-thick tissue sections were paraffinized and then routinely dewaxed in water before staining with Nissl body dye solution for 10 min. The stained sections were subjected to 95% alcohol dehydration and were sealed with neutral gum for examination using an Olympus light microscope (Japan) at × 400 magnification. Three random sections in three different fields were selected to count the number of apoptotic cells. Images were analyzed using Image-Pro Plus 6.0 software.

Statistical Analysis

Statistical analysis was performed using SPSS version 17.0 software (IBM SPSS Inc., Chicago, IL, USA). Data from at least three independent experiments are expressed as the mean ± standard deviation (SD). Comparisons between two groups were performed using the *t* test, and comparisons among more than two groups were performed using one-way ANOVA. Values of $p < 0.05$ were considered statistically significant.

RESULTS

Determination of Optimal PGN Concentration for Infecting Microglia and Optimal Time Points for Observing Autophagy Levels in Microglia

We tested three PGN concentrations (5 μg/ml, 15 μg/ml, and 30 μg/ml) to determine the optimal PGN concentration and the optimal time points of autophagy detection. Autophagy-associated proteins extracted from infected BV2 cells *in vitro* were analyzed using Western blot analysis at 12-h and 24-h culture time points. Autophagy was significantly increased at the 24-h time point compared to the 12-h time point. In addition, the 15 μg/ml PGN concentration induced the highest autophagy expression ($^*p < 0.05$) and showed a comparable autophagy level to that of 30 μg/ml PGN (Fig. 1). Thus, 15 μg/ml PGN and

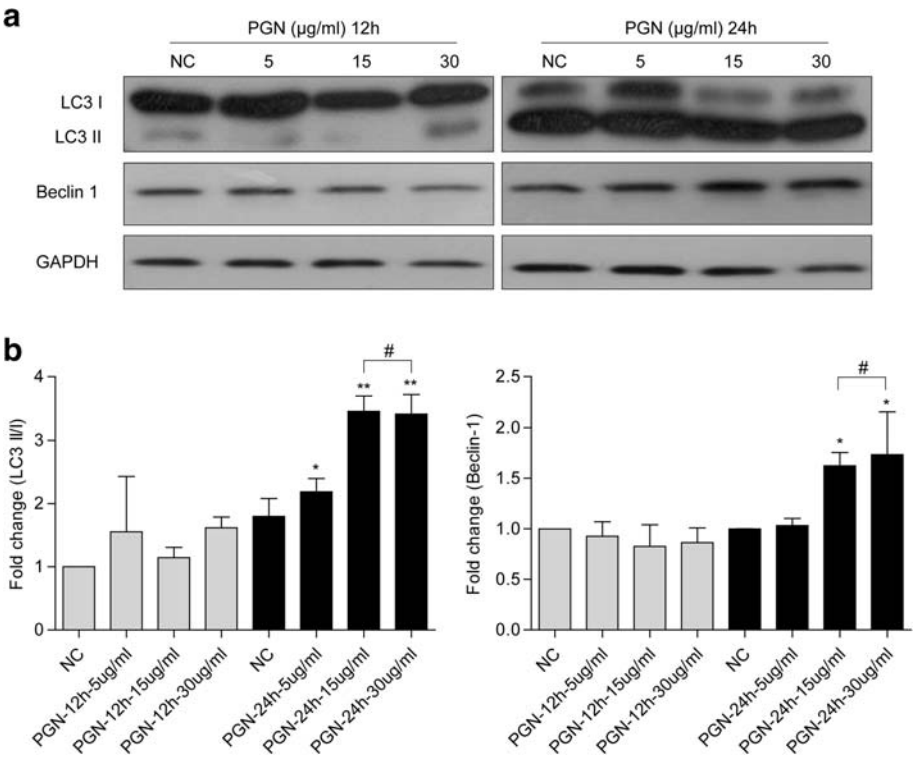

Fig. 1. Autophagy levels in PGN-activated microglia. **a** Western blot images of autophagy-associated proteins in BV2 cells treated with different PGN concentrations (5 μg/ml, 15 μg/ml, and 30 μg/ml) at 12-h and 24-h culture time points. **b** Semiquantitative profiles of LC3I/II and Beclin-1 protein expression at various PGN concentrations and culture detection time points. Data are presented as the mean ± SD; $n = 3$; $^{*}p < 0.05$; $^{**}p < 0.01$; $^{\#}p > 0.05$ *vs.* control.

detection at 24 h were selected for use in subsequent experiments.

Selection of the siRNA Sequence to Produce TLR2-KO

The siRNA sequence for TLR2-KO was selected from three different siRNA sequences that were each transfected into BV2 cells. TLR2 protein expression in the BV2 cells after siRNA treatment was assessed using Western blot analysis after 48 h of culture, with GAPDH as the loading control (Fig. 2a). The third siRNA sequence (si-TLR2-3) was selected for subsequent experiments, as it induced a 4-fold reduction in TLR2 expression compared to the other siTLR2 sequences ($^{**}p < 0.01$).

PGN Infection Activates TLR2 Signaling and Increases Autophagy in Microglia

To study the relationship between the autophagy level and the TLR2 pathway, the TLR2-specific ligand PGN was added to activate the pathway. Western blot analysis was performed to detect the expression of autophagy-associated proteins LC3I/II and Beclin-1 at the 24-h culture time point in the presence (PGN and PGN + TLR2-KO groups) or absence (negative control (NC) and TLR2-KO groups) of PGN (Fig. 2b), and immunofluorescence enabled observation of GFP-LC3 autophagic plaques (Fig. 2c). Higher autophagy (increased number of autophagic plaques) was observed in the PGN group ($^{**}p < 0.01$) but not in the TLR2-KO group ($^{\#}p > 0.05$) compared to the control group. This result indicates that PGN enhances autophagy by activating the TLR2 pathway.

TLR2-Mediated Autophagy Regulates Microglial Survival Through Microglial Phenotypic Switching

We used the TLR2 antagonist CU-CPT22 and agonist Pam3CSK4 to determine the effect of autophagy on microglial phenotypic transition and cell survival status. Immunofluorescence revealed no significant difference in TLR2 protein expression in the PGN group after the 24-h culture time point (Fig. 3a). However, a significant increase in TLR2 protein expression was observed in the PGN + Pam3CSK4 group, while a significant reduction in TLR2 protein expression was noted in the PGN + CU-CPT22

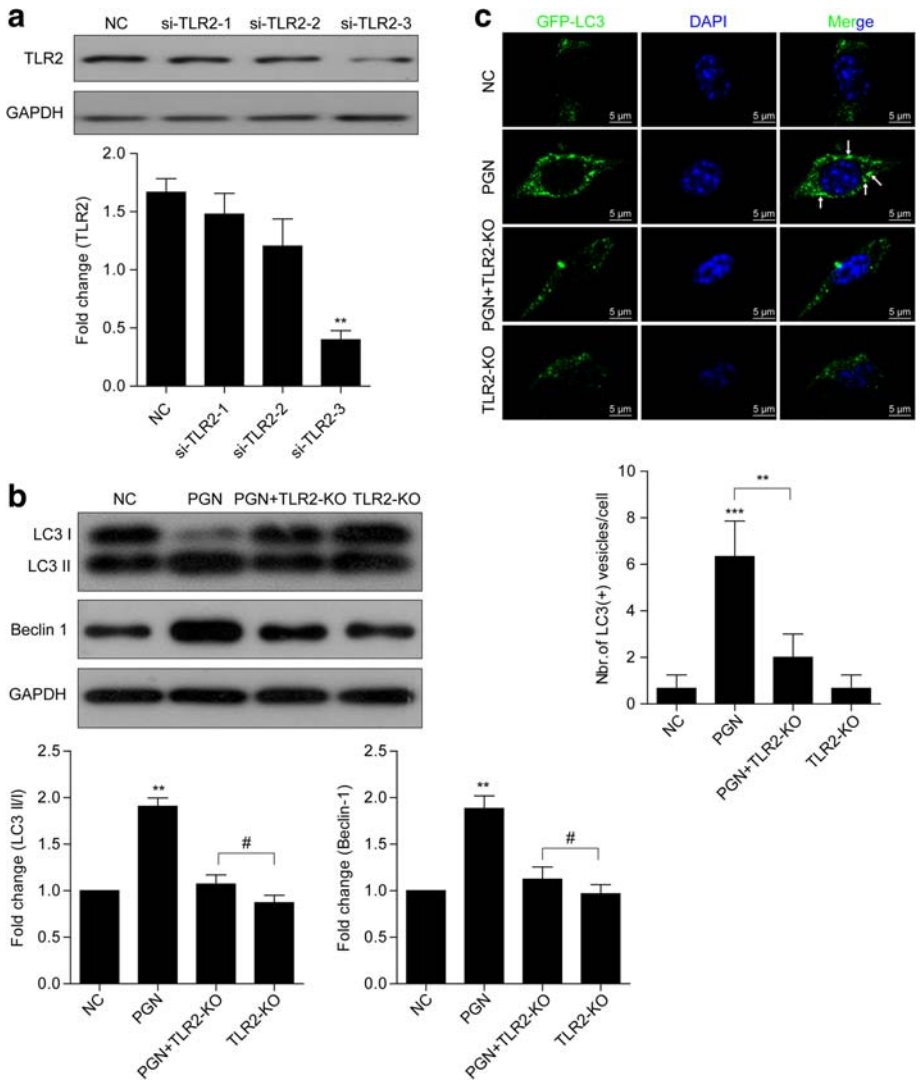

Fig. 2. PGN-induced autophagy in microglia is TLR2-dependent. Western blot images and semiquantitative profiles of LC3I/II and Beclin-1 protein levels **a** in BV2 cells transfected with the three tested TLR2 siRNA sequences (si-TLR2-1, si-TLR2-2, and si-TLR2-3) and **b** in the negative control (NC), PGN, PGN + si-TLR2, and si-TLR2 groups co-cultured with 15 μg/ml PGN for 24 h. **c** Confocal micrographs showing GFP-LC3 expression in microglia at the 24-h culture detection time point and corresponding histogram showing the average number of single $LC3^+$ autophagosomes detected from three independent experiments. Data are presented as the mean ± SD; $n = 3$; $^{**}p < 0.01$; $^{***}p < 0.001$; $^{\#}p > 0.05$ *vs.* control.

group. In addition, higher expression of autophagy markers LC3II and Beclin-1 was observed in the PGN + Pam3CSK4 group compared to the PGN group, while decreased autophagy marker expression was noted in the PGN + CU-CPT22 group. The expression levels of the M1-specific marker CD86 and the M1-associated cytokines TNF-α and IL-6, as well as the M2-specific marker CD206 and the M2-associated cytokines IL-10 and Arg-1, were assessed using ELISA at the 24-h culture time point (Fig. 3b). Increased autophagy and secretion of pro-inflammatory cytokines, but no change in the expression of cell markers, were observed in the PGN group. Similarly, we found increased autophagy and pro-inflammatory marker expression with obvious transition to the M1 phenotype and inhibition of M2 markers in the PGN + Pam3CSK4 group. The reverse was observed in the PGN + CU-CPT22 group, wherein microglia switched to the M2 phenotype with a concomitant decrease in M1-related protein expression ($^{*}p < 0.05$; $^{**}p < 0.01$). Using LC3B (green) and LAMP-1 (red) immunofluorescence assays,

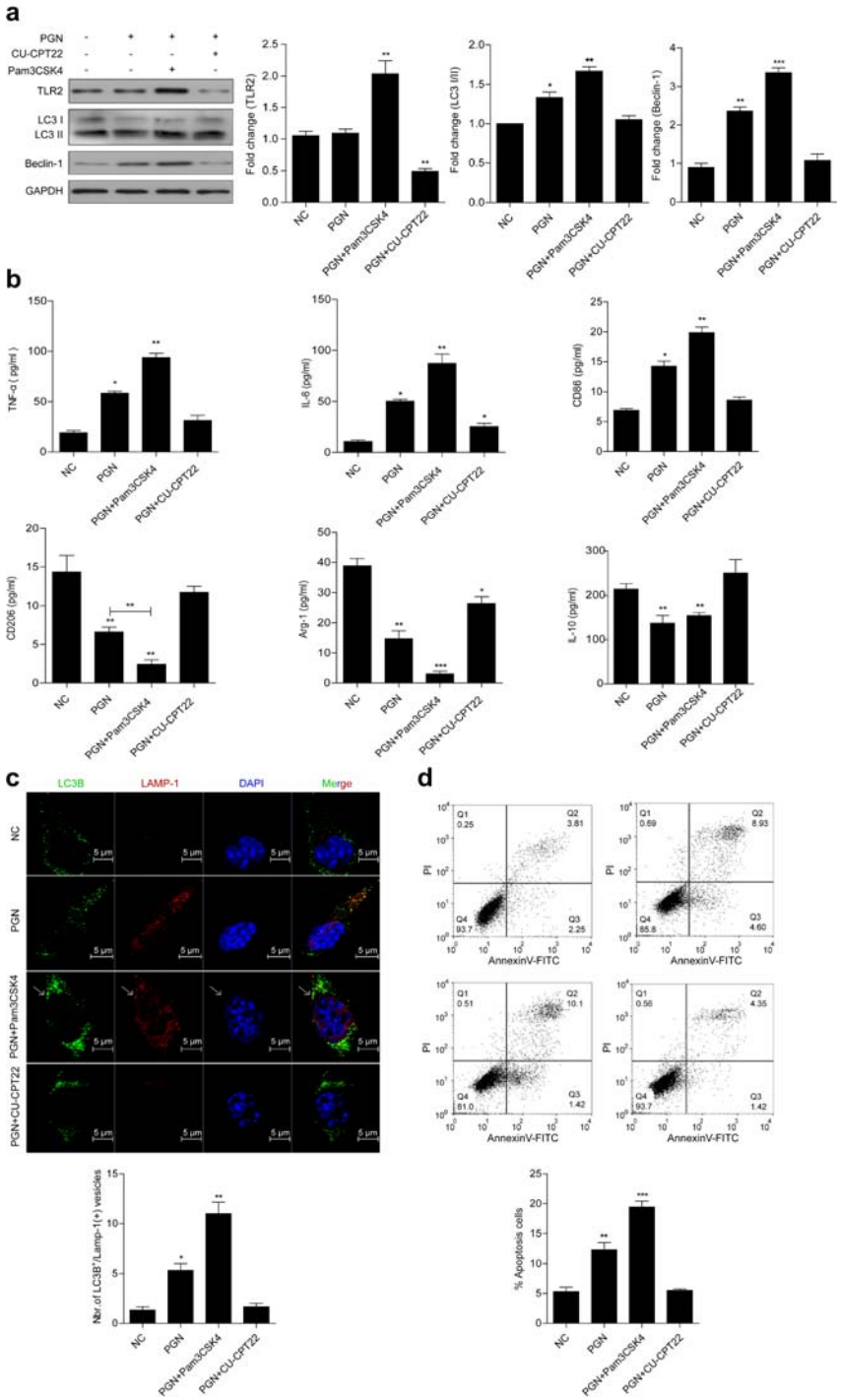

Fig. 3. TLR2-mediated autophagy regulates microglial phenotypic switching, which affects cell survival. **a** Western blot images and semiquantitative profiles of TLR2, LC3II/I, and Beclin-1 protein levels in BV2 cells co-cultured with 15 μg/ml PGN for 24 h at 37 °C supplemented with 50 nM Pam3CSK4 or 10 μM CU-CPT22. **b** ELISA profiles of M1-associated markers (CD86, TNF-α, and IL-6) and M2-associated markers (CD206, Arg-1, and IL-10). **c** Confocal images showing LC3B (green) and LAMP-1 (red) co-localization at the 24-h culture time point and a histogram of the number of co-localized LC3B/LAMP-1-labeled autophagosomes in the four groups: NC, PGN + CU-CPT22, PGN, and PGN + Pam3CSK4. **d** Flow cytometry profiles showing the level of apoptosis in the four groups of BV2 cells tested. Data are presented as the mean ± SD; $n = 3$; $^{*}p < 0.05$; $^{**}p < 0.01$; $^{***}p < 0.001$ *vs.* control.

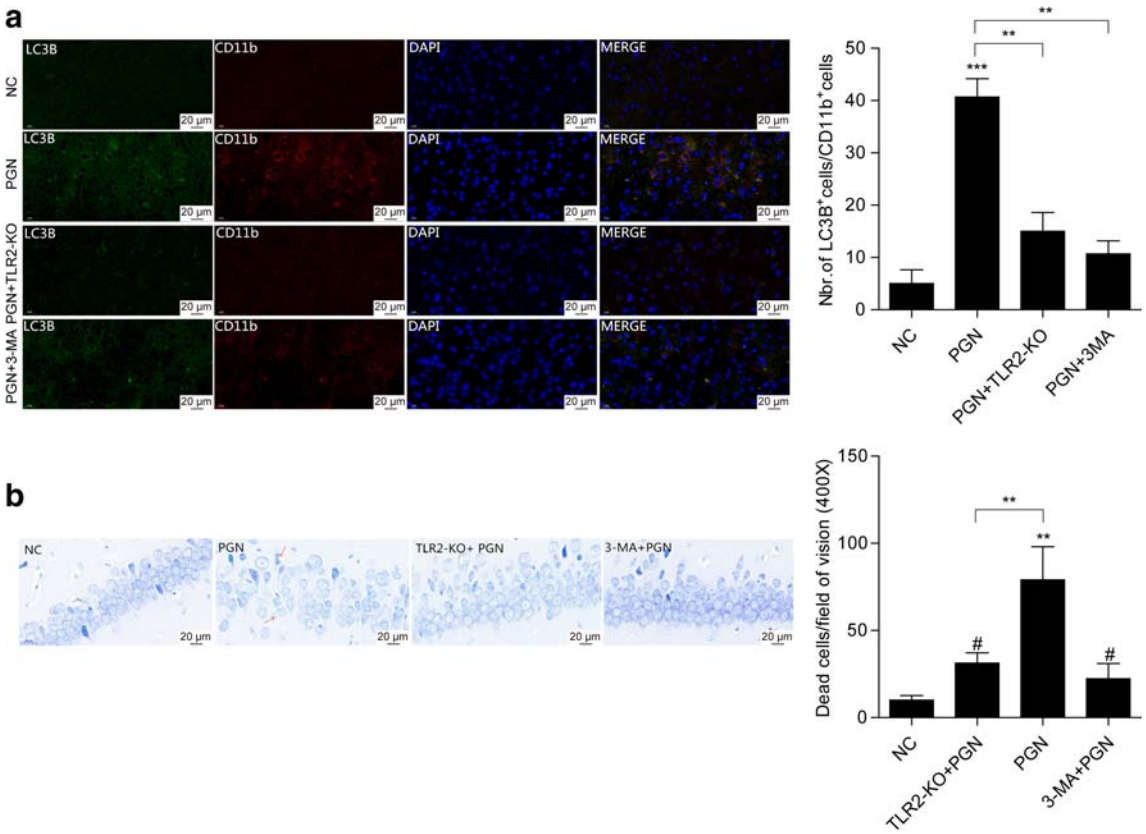

Fig. 4. The effect of autophagy on microglial survival in PGN-treated mice. **a** Confocal fluorescence images at × 400 magnification showing LC3B (green) and CD11b (red) co-localization in NC, PGN, PGN + TLR2-KO, and PGN + 3-MA mice at the 48-h culture time point and the histogram representing the number of positively stained cells. $^{**}p < 0.01$; $^{***}p < 0.001$ *vs.* control. **b** Nissl staining images at × 400 magnification and the histogram of apoptotic cells in the mouse hippocampus. The same apoptotic microglial cells (red arrow) are shown in each selected field for counting and calculation of the average values. $^{\#}p < 0.05$; $^{**}p < 0.01$.

we observed an increased number of autophagosomes in the PGN and PGN + Pam3CSK4 groups (Fig. 3c). Flow cytometry showed that autophagy was enhanced with increased apoptosis (Fig. 3d), and the extent of apoptosis was consistent with M1 phenotypic switching.

Autophagy Is Associated with Microglial Damage and TLR2 Signaling

The number of autophagosomes was the highest in the microglia of the PGN group, and autophagy was significantly reduced in the TLR2-KO and 3-MA groups (Fig. 4a). Nissl bodies in normal microglia stained dark blue with toluidine blue dye, and the nuclei stained light blue, while damaged or apoptotic microglia were faintly stained or unstained. Damaged or apoptotic microglia were the most significant in the PGN group, unlike in the TLR2-KO and 3-MA groups, which showed more intense Nissl staining (Fig. 4b); these results indicated that enhanced autophagy can increase microglial damage and that TLR2 inhibition or 3-MA-induced autophagy inhibition confers cytoprotective effects on microglia.

DISCUSSION

Activation of microglial cells with bacterial PGN may result in the induction of microglial cell death by mechanisms involving autophagy both *in vitro* and *in vivo* [26]. In our present study, we found that PGN-stimulated microglial cells can significantly increase the expression of LC3-II and Beclin-1 after 24 h of co-culture, and the level of autophagy was positively correlated with PGN concentration, peaking at 15 μg/ml. Our Western blot analysis, immunofluorescence assays, and TLR2-KO

mouse model studies revealed that PGN was able to induce autophagy in microglia through the TLR2 signaling pathway.

To support our results at the transcriptional level, we selected the most effective siRNA sequence from among three sequences to knockdown expression of the TLR2 gene in microglia and establish effective TLR2 silencing. We analyzed the role of TLR2 in autophagy in PGN-stimulated microglia *in vitro*, and our results showed that knockdown of TLR2 by using siRNA markedly reduced the autophagic level compared to treatment with control siRNA. This result suggested that TLR2 plays a critical role in autophagy in PGN-stimulated microglia. Furthermore, we observed that knocking down TLR2 by siRNA significantly reduced the expression of LC3-II and Beclin-1 proteins and the number of GFP-LC3 punctate structures. Recently, other researchers have also demonstrated that induction of autophagy could be suppressed by TLR2 silencing [27, 28]. Indeed, in TLR2-KO cells *in vitro*, it has been demonstrated that knockdown of TLR2 led to decreased autophagy that was dependent on significantly reduced expression levels of LC3-II and Beclin-1 proteins [29, 30]. These results consistently demonstrated that the TLR2 signaling pathway is involved in autophagy activation. However, contrary to the findings of the present study, Poluzzi *et al.* reported that TLR4, and not TLR2, is the critical co-activator of M1 autophagy, along with CD44 [Poluzzi, 2019 citation]. Poluzzi *et al.* also demonstrated that the CD44/TLR4 signaling axis, and not TLR2, was the primary mediator of autophagy in biglycan-induced macrophages, as they examined the effect on autophagy after ischemia-reperfusion. Moreover, in the present study, we used the Gram-positive cocci cell wall component PGN, which is known to specifically activate TLR2, and not TLR4, that primarily recognizes Gram-negative bacilli, to enhance autophagy. Thus, these differences may account for the distinct conclusions made in the present study compared with the study of Poluzzi *et al.*

Recently, it was shown that microglia are a highly plastic cell population in the CNS that serve multiple roles not only in homeostasis of the CNS but also in recovery from pathological conditions [32, 33]. TLR2 plays a role in the host antibacterial immune response to both bacterial meningitis and brain abscesses [34, 35]. However, whether the TLR2 signaling pathway participates in autophagy of microglia following cerebral infection is unknown. Our Nissl staining and histoimmunofluorescence studies have shown a correlation between autophagy and TLR2 signaling pathways in the TLR2-KO model. We showed that PGN injection into the mouse brain triggered formation of $LC3B^+$ puncta in $CD11b^+$ cells, recruitment of leukocytes and phagocytes to the injection site, and damage to microglia. Moreover, these effects of PGN were reduced in TLR2-KO and 3-MA-treated mice as evidenced by the decreased autophagy, inflammatory cell recruitment, and microglial apoptosis. Previous studies have also found that PGN injection into the brain parenchyma triggered $LC3B^+$ puncta formation in $CD45^+$ cells, pro-inflammatory mediator production, and neurotoxicity [36]. Our findings are consistent with previous reports. This observation suggested that inhibition of these signaling pathways could reduce microglial activation and leukocyte recruitment, thereby enabling neuroprotection.

Autophagy can be viewed as a double-edged sword. Autophagy is protective when activated by mild physiological stressors; however, over-activation of autophagy can lead to a series of fatal consequences [37, 38]. Researchers have found that both over-activation and inactivation of autophagy can lead to neuronal death [39, 40]. However, the mechanism influencing the effect of TLR2-mediated autophagy on microglial survival is unknown. Our immunofluorescence assays and ELISA analysis have confirmed that autophagy is involved in microglial M1/M2 phenotypic switching, and it regulates microglial survival. Pam3CSK4 treatment significantly increased the level of LC3B/LAMP-1 fluorescence co-localization compared to PGN treatment alone, and over-activation of autophagy promoted high expression of the M1 phenotypic marker CD86 and pro-inflammatory mediators, such as TNF-α and IL-6, while the TLR2 antagonist CU-CPT22 treatment inhibited the expression of M1 markers and upregulated the level of M2 phenotypic marker CD206 and anti-inflammatory mediators, such as IL-10 and Arg-1. In addition, using flow cytometry, we found that the TLR2 agonist increased microglial apoptosis, whereas the TLR2 antagonist significantly reduced microglial apoptosis, compared to PGN treatment alone. Animal studies have also shown that TLR2-KO mice or 3-MA-treated mice had decreased autophagy and reduced microglial apoptosis following cerebral infection. These results indicate that over-activation of autophagy is responsible for the M1 polarization of microglia and promotes microglial apoptosis. Indeed, the effects of autophagy on the microglial phenotype are different under various pathological conditions. Other studies have reported that inhibition of autophagic flux induced an M1 microglial phenotype following oxygen-glucose deprivation/reperfusion in BV2 cells, with high levels of TNF-α, iNOS, and COX-2 [3]. In addition, upregulation of autophagy promoted microglia towards an M2 phenotype while inhibition of autophagy increased the

M1 polarization associated with neurodegenerative diseases [41, 42]. These studies demonstrated the multifaceted nature of autophagy under different pathological conditions. In summary, our results first suggested that an inhibited autophagic flux induced an M2 microglial phenotype following infection, and this phenomenon promoted microglial survival.

In conclusion, our studies have shown that TLR2 deficiency or inhibition of autophagy contributes to enhanced neuroprotective properties in PGN-induced microglia. Moreover, TLR2-mediated autophagy could regulate microglial M1/M2 phenotype switching. Overactivation of autophagy promoted microglial M1 polarization and increased apoptosis. Inhibition of autophagy induced microglial polarization towards the M2 phenotype, decreased the inflammatory response, and, in turn, promoted neuroprotection. Our studies suggest that modulating autophagy-regulated M1/M2 polarization may be a potential strategy for treating neuroinflammation-related disorders. These findings may have revealed a novel immune regulatory mechanism that links the innate immune receptor TLR2 and autophagy-regulated M1/M2 polarization after infection.

AUTHOR CONTRIBUTIONS

Xinjie Liu: study conception and design; Kun Ma: experiments and manuscript writing; Jingjing Guo: data collection and analysis; Guan Wang and Qiuying Ni: material preparation and data collection

All authors read and approved the final manuscript.

FUNDING INFORMATION

This work was supported by the National Natural Science Foundation (Project no. 31571557).**DATA AVAILABILITY**

The data that support the findings of this study are available from the corresponding author upon reasonable request.**COMPLIANCE WITH ETHICAL STANDARDS**

Conflict of Interest. The authors declare that they have no conflict of interest.

Ethical Approval. The experiments complied with the Regulations of the Administration of Laboratory Animals of the Ministry of Health of China (Document No. 55 of 2001) and were approved by the Animal Ethics Committee of Shandong University, China.

REFERENCES

1. McWhorter, F.Y., T. Wang, P. Nguyen, T. Chung, and W.F. Liu. 2013. Modulation of macrophage phenotype by cell shape. *Proceedings of the National Academy of Sciences of the United States of America* 110 (43): 17253–17258.
2. Kobayashi, K., S. Imagama, T. Ohgomori, K. Hirano, K. Uchimura, K. Sakamoto, et al. 2013. Minocycline selectively inhibits M1 polarization of microglia. *Cell Death & Disease* 4: e525.
3. Xia, C.Y., S. Zhang, S.F. Chu, Z.Z. Wang, X.Y. Song, W. Zuo, Y. Gao, P.F. Yang, and N.H. Chen. 2016. Autophagic flux regulates microglial phenotype according to the time of oxygen-glucose deprivation/reperfusion. *International Immunopharmacology* 39: 140–148.
4. Hu, X., R.K. Leak, Y. Shi, J. Suenaga, Y. Gao, P. Zheng, and J. Chen. 2015. Microglial and macrophage polarization-new prospects for brain repair. *Nature Reviews. Neurology* 11 (1): 56–64.
5. Yao, X., S. Liu, W. Ding, P. Yue, Q. Jiang, M. Zhao, et al. 2017. TLR4 signal ablation attenuated neurological deficits by regulating microglial M1/M2 phenotype after traumatic brain injury in mice. *Journal of Neuroimmunology* 310: 38–45.
6. Machado-Pereira, M., T. Santos, L. Ferreira, L. Bernardino, and R. Ferreira. 2017. Anti-inflammatory strategy for M2 microglial polarization using retinoic acid-loaded nanoparticles. *Mediators of Inflammation* 2017: 6742427.
7. Nicolas, S., J. Cazareth, H. Zarif, A. Guyon, C. Heurteaux, J. Chabry, et al. 2017. Globular adiponectin limits microglia pro-inflammatory phenotype through an AdipoR1/NF-kappaB signaling pathway. *Frontiers in Cellular Neuroscience* 11: 352.
8. Zhou, T., Z. Huang, X. Sun, X. Zhu, L. Zhou, M. Li, et al. 2017. Microglia polarization with M1/M2 phenotype changes in rd1 mouse model of retinal degeneration. *Frontiers in Neuroanatomy* 11: 77.
9. Aryanpour, R., P. Pasbakhsh, K. Zibara, Z. Namjoo, F. Beigi Boroujeni, S. Shahbeigi, et al. 2017. Progesterone therapy induces an M1 to M2 switch in microglia phenotype and suppresses NLRP3 inflammasome in a cuprizone-induced demyelination mouse model. *International Immunopharmacology* 51: 131–139.

10. Qin, C., W.H. Fan, Q. Liu, K. Shang, M. Murugan, L.J. Wu, W. Wang, and D.S. Tian. 2017. Fingolimod protects against ischemic white matter damage by modulating microglia toward M2 polarization via STAT3 pathway. *Stroke* 48 (12): 3336–3346.
11. Bussi, C., J.M. Peralta Ramos, D.S. Arroyo, E.A. Gaviglio, J.I. Gallea, J.M. Wang, et al. 2017. Autophagy down regulates pro-inflammatory mediators in BV2 microglial cells and rescues both LPS and alpha-synuclein induced neuronal cell death. *Scientific Reports* 7: 43153.
12. He, Y., H. She, T. Zhang, H. Xu, L. Cheng, M. Yepes, Y. Zhao, and Z. Mao. 2018. p38 MAPK inhibits autophagy and promotes microglial inflammatory responses by phosphorylating ULK1. *The Journal of Cell Biology* 217 (1): 315–328.
13. Mizushima, N., and M. Komatsu. 2011. Autophagy: Renovation of cells and tissues. *Cell* 147 (4): 728–741.
14. Carneiro, L.A., and L.H. Travassos. 2013. The interplay between NLRs and autophagy in immunity and inflammation. *Frontiers in Immunology* 4: 361.
15. Kim, J.Y., J.C. Paton, D.E. Briles, D.K. Rhee, and S. Pyo. 2015. Streptococcus pneumoniae induces pyroptosis through the regulation of autophagy in murine microglia. *Oncotarget* 6 (42): 44161–44178.
16. Guo, J.Y., B. Xia, and E. White. 2013. Autophagy-mediated tumor promotion. *Cell* 155 (6): 1216–1219.
17. Mehrpour, M., A. Esclatine, I. Beau, and P. Codogno. 2010. Overview of macroautophagy regulation in mammalian cells. *Cell Research* 20 (7): 748–762.
18. Jiang, P., and N. Mizushima. 2014. Autophagy and human diseases. *Cell Research* 24: 69–79.
19. Nixon, R.A., and D.S. Yang. 2011. Autophagy failure in Alzheimer's disease—locating the primary defect. *Neurobiology of Disease* 43 (1): 38–45.
20. Saitoh, T., and S. Akira. 2010. Regulation of innate immune responses by autophagy-related proteins. *The Journal of Cell Biology* 189 (6): 925–935.
21. Su, P., J. Zhang, D. Wang, F. Zhao, Z. Cao, M. Aschner, and W. Luo. 2016. The role of autophagy in modulation of neuroinflammation in microglia. *Neuroscience* 319: 155–167.
22. Ribes, S., S. Ebert, T. Regen, A. Agarwal, S.C. Tauber, D. Czesnik, et al. 2010. Toll-like receptor stimulation enhances phagocytosis and intracellular killing of nonencapsulated and encapsulated Streptococcus pneumoniae by murine microglia. *Infection and Immunity* 78 (2): 865–871.
23. Hug, H., M.H. Mohajeri, and G. La Fata. 2018. Toll-like receptors: Regulators of the immune response in the human gut. *Nutrients* 10 (2).
24. Liu, X., Q. Han, and J. Leng. 2014. Analysis of nucleotide-binding oligomerization domain proteins in a murine model of pneumococcal meningitis. *BMC Infectious Diseases* 14: 648.
25. Texereau, J., J.D. Chiche, W. Taylor, G. Choukroun, B. Comba, and J.P. Mira. 2005. The importance of Toll-like receptor 2 polymorphisms in severe infections. *Clinical Infectious Diseases* 41 (Suppl 7): S408–S415.
26. Arroyo, D.S., J.A. Soria, E.A. Gaviglio, C. Garcia-Keller, L.M. Cancela, M.C. Rodriguez-Galan, J.M. Wang, and P. Iribarren. 2013. Toll-like receptor 2 ligands promote microglial cell death by inducing autophagy. *The FASEB Journal* 27 (1): 299–312.
27. Fang, L., H.M. Wu, P.S. Ding, and R.Y. Liu. 2014. TLR2 mediates phagocytosis and autophagy through JNK signaling pathway in Staphylococcus aureus-stimulated RAW264.7 cells. *Cellular Signalling* 26 (4): 806–814.
28. Shin, D.M., J.M. Yuk, H.M. Lee, S.H. Lee, J.W. Son, C.V. Harding, J.M. Kim, R.L. Modlin, and E.K. Jo. 2010. Mycobacterial lipoprotein activates autophagy via TLR2/1/CD14 and a functional vitamin D receptor signalling. *Cellular Microbiology* 12 (11): 1648–1665.
29. Lu, Z., D. Xie, Y. Chen, E. Tian, I. Muhammad, X. Chen, Y. Miao, W. Hu, Z. Wu, H. Ni, J. Xin, Y. Li, and J. Li. 2017. TLR2 mediates autophagy through ERK signaling pathway in Mycoplasma gallisepticum-infected RAW264.7 cells. *Molecular Immunology* 87: 161–170.
30. Shen, Q., X. Zhang, Q. Li, J. Zhang, H. Lai, H. Gan, X. du, and M. Li. 2019. TLR2 protects cisplatin-induced acute kidney injury associated with autophagy via PI3K/Akt signaling pathway. *Journal of Cellular Biochemistry* 120 (3): 4366–4374.
31. Poluzzi, C., M.V. Nastase, J. Zeng-Brouwers, H. Roedig, L.T. Hsieh, J.B. Michaelis, et al. 2019. Biglycan evokes autophagy in macrophages via a novel CD44/Toll-like receptor 4 signaling axis in ischemia/reperfusion injury. *Kidney Int* 95 (3): 540–562.
32. Masuda, T., and M. Prinz. 2016. Microglia: A unique versatile cell in the central nervous system. *ACS Chemical Neuroscience* 7 (4): 428–434.
33. Liu, X., V.S. Chauhan, A.B. Young, and I. Marriott. 2010. NOD2 mediates inflammatory responses of primary murine glia to Streptococcus pneumoniae. *Glia* 58 (7): 839–847.
34. Kielian, T., and W.F. Hickey. 2000. Proinflammatory cytokine, chemokine, and cellular adhesion molecule expression during the acute phase of experimental brain abscess development. *The American Journal of Pathology* 157 (2): 647–658.
35. Kielian, T., A. Haney, P.M. Mayes, S. Garg, and N. Esen. 2005. Toll-like receptor 2 modulates the proinflammatory milieu in Staphylococcus aureus-induced brain abscess. *Infection and Immunity* 73 (11): 7428–7435.
36. Arroyo, D.S., E.A. Gaviglio, J.M. Peralta Ramos, C. Bussi, M.P. Avalos, L.M. Cancela, et al. 2018. Phosphatidyl-inositol-3 kinase inhibitors regulate peptidoglycan-induced myeloid leukocyte recruitment, inflammation, and neurotoxicity in mouse brain. *Frontiers in Immunology* 9: 770.
37. Xin, X.Y., J. Pan, X.Q. Wang, J.F. Ma, J.Q. Ding, G.Y. Yang, and S.D. Chen. 2011. 2-Methoxyestradiol attenuates autophagy activation after global ischemia. *The Canadian Journal of Neurological Sciences* 38 (4): 631–638.
38. Wang, P., Y.F. Guan, H. Du, Q.W. Zhai, D.F. Su, and C.Y. Miao. 2012. Induction of autophagy contributes to the neuroprotection of nicotinamide phosphoribosyltransferase in cerebral ischemia. *Autophagy* 8 (1): 77–87.
39. Button, R.W., S. Luo, and D.C. Rubinsztein. 2015. Autophagic activity in neuronal cell death. *Neuroscience Bulletin* 31 (4): 382–394.
40. Ginet, V., M.P. Pittet, C. Rummel, M.C. Osterheld, R. Meuli, P.G. Clarke, et al. 2014. Dying neurons in thalamus of asphyxiated term newborns and rats are autophagic. *Annals of Neurology* 76 (5): 695–711.
41. Moehle, M.S., and A.B. West. 2015. M1 and M2 immune activation in Parkinson's disease: Foe and ally? *Neuroscience* 302: 59–73.
42. Jin, M.M., F. Wang, D. Qi, W.W. Liu, C. Gu, C.J. Mao, et al. 2018. A critical role of autophagy in regulating microglia polarization in neurodegeneration. *Frontiers in Aging Neuroscience* 10: 378.